Journal of Virology

| Editor's Pick | Bacteriology | Minireview

Many paths, similar destinations: viruses and bacterial microcompartments form polyhedra inside cells

Kristin N. Parent,[1] **Cheryl A. Kerfeld**[1,2,3,4]

AUTHOR AFFILIATIONS See affiliation list on p. 10.

ABSTRACT A large number of biological entities assemble into icosahedral structures, and these are ubiquitous throughout nature. Examples include eukaryotic and prokaryotic viral capsids and more recently discovered bacterial microcompartments. Viral capsids and bacterial microcompartments are both composed of pentameric and hexameric subunits; however, they differ in the type of cargo they encapsulate: nucleic acid or protein. Also, both depart from strict icosahedral symmetry: while this is less common in viruses, among bacterial microcompartments, diverse and heterogeneous polyhedra are common. We review shared principles and key distinctions between the self-directed assembly of various icosahedral architectures and their polyhedral variants in nature and explore the concept that there are multiple paths, influenced by their cargo, to arriving at similar protein cage morphologies.

KEYWORDS bacteriophage, virus, carboxysome, encapsulins, bacterial microcompartments

Icosahedral proteinaceous shells are important containers for many biological functions. These shells are capable of self-directed assembly from one or a few subunits, are relatively optimal in surface to volume ratio, and are inherently stable and robust to protect their internal cargo. Understanding shell properties is crucial for a number of disciplines. In virology, many capsids are icosahedral and protect the genetic cargo from environmental onslaughts and host defense mechanisms. Understanding the structure and assembly pathways of viral shells can guide rational drug design, vaccine development, receptor or immune-antibody-binding studies, etc. (1, 2). For bacterial microcompartments (BMCs), these shells both cluster and protect segments of both anabolic (carboxysome) and catabolic (metabolosome) pathways. BMC shells also provide selective permeability for the exchange of metabolites with the bulk environment. Encapsulins are classified as bacterial nanocompartments and are distinct from BMCs. Encapsulins serve diverse functions, with roles in stress response, iron storage, and detoxification, to name a few (3, 4). Understanding BMC and encapsulin structures can inform us about the diverse functions of these shells in nature, and this knowledge can be used to guide the design of synthetic BMCs for bioengineering (5) and biomedical (6) applications.

Scalability of shells: how to build bigger icosahedra and triangulation number

An icosahedron is simply a spherical structure with 12 vertices and 20 angular facets. Consider the classic organization of a soccer ball, with the black pentagonal shapes and the white hexagonal shapes. The simplest of these structures can be built from 60 subunits into a so-called Triangulation number 1 ("T=1") assembly consisting entirely of pentagonal shapes. Bigger structures can be assembled by the addition of hexagonal shapes progressively into T=3, T=4, T=7….T=52 complexes, etc., according to this

Editor Suchetana Mukhopadhyay, Indiana University Bloomington, Bloomington, Indiana, USA

Address correspondence to Kristin N. Parent, kparent@msu.edu.

The authors declare no conflict of interest.

See the funding table on p. 10.

Published 20 April 2026

equation: $T=h^2+hk+k^2$ (7). In this relationship, *h* and *k* define the complexity of the icosahedron and can be used to index the structure. The structure can be described as taking *h* steps away from a penton vertex and then taking *k* steps to get to the next fivefold vertex. In biology, pentagonal and hexagonal shapes are most often formed from individual protein chains that assemble into pentameric oligomers (five protein subunits) and hexameric oligomers (six protein subunits) used to build icosahedral particles. The T number can also be described as a multiple of 60 protein subunits (e.g., a T=3 capsid has 60*3, or 180 subunits, and a T=4 capsid has 60*4, or 240 units, etc.).

Bacteriophages, eukaryotic viruses (8), and bacterial microcompartments (9, 10) are examples of natural protein cages that can be formed with icosahedral symmetry but also depart from perfect symmetry to form other polyhedra. In this review, we will focus on the protein subunits, assembly pathways, and principles of forming biological shells, mainly focusing on viruses and bacterial microcompartments.

THE BUILDING BLOCKS OF THE SHELLS OF VIRUSES AND BACTERIAL MICROCOMPARTMENTS

Common structures: shell building blocks use a minimal number of folds

The vast majority of viruses are icosahedra, formed from chemically identical protein subunits that can adopt different local configurations to accommodate pentameric and hexameric oligomerization according to the Caspar Klug theory of quasi equivalence (7). This has been extensively studied using a number of model systems. The first high-resolution structure of a bacteriophage capsid was from X-ray crystallography studies on the Hong Kong 97 phage capsid (11, 12). This has since become the namesake of this protein family (i.e., the "HK97 fold"). Proteins with the HK97 fold are not the only ones capable of building icosahedral structures in virology. There are currently four known common folds that drive capsid assembly in viral systems that span across domains of life, including examples within bacteria, archaea, and eukaryota (13), and each viral family has a shared fold among their members (Fig. 1). These four folds encompass (i) the HK97 fold across all known dsDNA containing tailed bacteriophages and the herpesviruses, (ii) the Bluetongue virus-like fold ("BTV-like") common among dsRNA viruses, (iii) the PRD1/adenovirus lineage ("PRD1-like") that spans larger dsDNA viruses such as adenoviruses and giant viruses, as well as some phages, and the (4) picornovirus-like fold for small ssRNA viruses, dsDNA such as SV40 and papillomavirus, and ssDNA viruses such as parvoviruses (13–16).

Forming icosahedra from limited subunit types: efficient use of genome space

Studies on related phages such as bacteriophage P22 have also shed light on capsid assembly (18, 19). Phages like HK97 and P22 have ~40 kb genomes, and their capsids assemble into T=7 isometric cages (of ~50 nm diameter) from a single gene product called the major coat protein. Using the same building block for both hexons and pentons makes efficient use of genomic space since smaller viruses can only package a finite amount of genomic material. Rarely, some phages and viruses assemble from chemically distinct protein subunits derived from the expression of multiple genes. In these cases, one type of protein forms oligomers with cyclic fivefold symmetry called pentons, while a second protein forms cyclic oligomers with sixfold symmetry called hexons. Bacteriophage T4 falls into this category, where the hexons are formed from gp23 protein while the pentons are formed from gp24 protein (20). By comparison to HK97 or P22, phage T4 has a much larger genome (~145 kbp), a larger capsid organized into a prolate T=13 geometry, and a capsid size of 120 nm by 86 nm (21). Phage T4 can therefore more easily accommodate multiple genes encoding different capsid proteins. Another way of maximizing the efficiency of genomic space is achieved by eukaryotic viruses that assemble from two or three subunit types created from a single gene by either post-translational modifications, such as proteolytic cleavage seen in the processing of VP0 in polio (22, 23), or via translational regulation (e.g., alternative start sites observed in systems such as adeno-associated viruses [24] and polyomaviruses [25]).

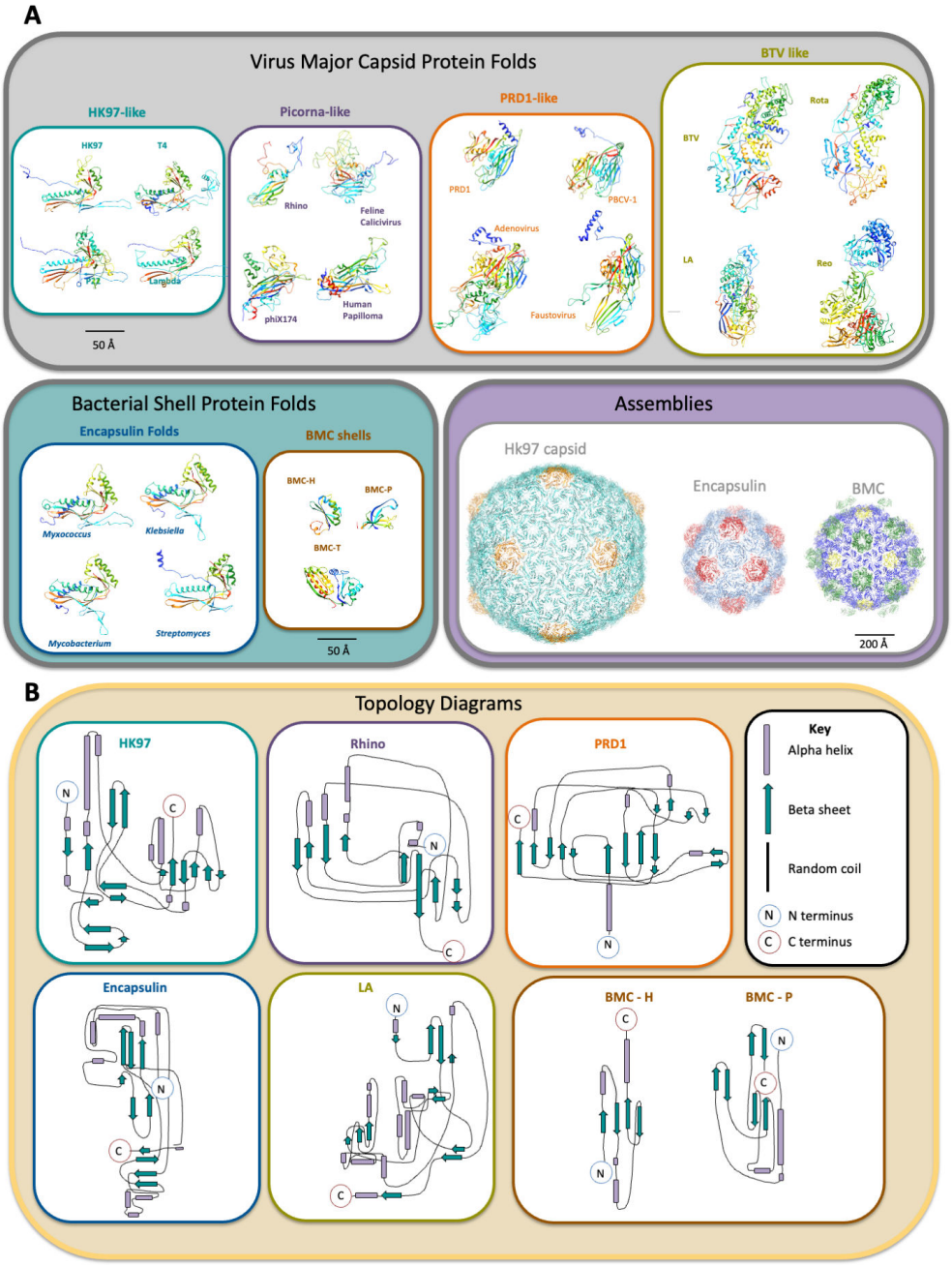

FIG 1 Structural comparison of a variety of biological icosahedra: Viruses and bacterial shells. (A) Examples of monomers from viruses are grouped according to the four known viral folds. Each monomer is colored from the N-terminus (blue) to the C-terminus (red). Both HK97 and encapsulins share a homologous fold, whereas the BMC shell proteins are unrelated. The HK97 fold group includes all known dsDNA-containing tailed phages and herpesviruses. Representatives are bacteriophages HK97 (PDB 1OHG), Phage T4 (PDB 1YUE), Phage P22 (PDB 8I1T), and Phage Lambda (PDB 7VIK). The picornavirus group includes small ssRNA and small ssDNA viruses such as rhinovirus-B5 (PDB 6SK6), Feline Calicivirus (PDB 3M8L), *Microviridae* member phage phiX174 (PDB 9K3M), and human papillomavirus (PDB 2R5K). The PRD1-like group spans larger dsDNA viruses such as adenoviruses, tailless dsDNA containing icosahedral phages, and giant viruses. Representatives are Phage PRD1 (PDB 1CJD), Cholovirus PBCV-1 (PDB 5TIP), adenovirus (PDB 1P30), and giant virus Fausovirus (PDB 5J7O). The Bluetongue virus group (BTV-like) includes dsRNA viruses such as BTV (PDB 2BTV), rotavirus (PDB 3KZ4), L-A virus (PDB 1M1C), and reovirus (PDB 1EJ6). Examples of monomers from a variety of encapsulins, including *Myxococcus xanthus* EncA (PDB 8VJO), *Klebsiella pneumoniae* DyP peroxidase (PDB 8U50), *Mycobacterium smegmatis* encapsulating shell (PDB 7BOJ), and *Streptomyces lydicus* Encapsulin 1 (PDB 9BJE): note the structural homology to the viral proteins in the HK97-like group. By comparison, bacterial

(Continued on next page)

Fig 1 (Continued)

microcompartment shell protein monomers have a distinct topology. The structures of BMC-H (hexamer), BMC-P (pentamer), and BMC-T (trimer) proteins from *Haliangium ochraceum* (HO) microcompartment shells (PDB 5V74). Assemblies of these monomers into icosahedral shells are also shown for HK97, *M. xanthus encapsulin*, and HO shells. Hexons and pentons are rendered in different colors. (B) Topology diagrams of a representative protein from each cluster of folds, generated with Pro-Origami (17).

While viral pentons and hexons can form from either chemically identical monomers in a quasi-equivalent conformation (most phages and herpesviruses), or from distinct protein subunits (such as phage T4, polio, and adeno-associated viruses, etc.), in general, the core unit of the monomers retains the same overall fold. For example, the HK97-fold is ubiquitous among all known dsDNA-containing bacteriophage and herpesviruses and is quite versatile for assembly into a large array of capsid sizes ranging in sizes from 50 to 180 nm diameters while maintaining the rules of icosahedral symmetry (26, 27).

Similarly, subcellular encapsulins form nanocages to compartmentalize biochemical reactions from chemically and structurally identical subunits (28). Two examples include the iron-storing encapsulin in *Myxococcus xanthus* (29), and peroxidase encapsulins in enterobacteria (30). These encapsulins form cages from bacterially encoded proteins that are structurally homologous to the phage HK97 major coat protein (Fig. 1). There are now thousands of bioinformatically identified encapsulin systems across bacteria and archaea; all maintain the HK97 fold as their building blocks (31). There is a strong evolutionary relationship between encapsulins and bacteriophages, likely acquiring the same protein fold through horizontal gene transfer (32, 33). Generally, encapsulin assembly is high fidelity in native systems, but heterogeneous structure deviations occur when cargo loading is greatly enhanced (34).

In contrast, BMCs, which are organelles that compartmentalize segments of metabolic pathways in shells, are formed from hexagonal and pentagonal protein oligomers formed by distinct protein families. The Pfam 00936 domain forms hexameric (BMC-H proteins) or trimeric (BMC-T proteins) oligomers structurally comparable to hexons, and the Pfam 03319 domain (BMC-P proteins) that form pentameric oligomers (Fig. 2). These protein families are unrelated to any known viral proteins, but are shared among all functionally diverse BMCs. Moreover, unlike viruses and encapsulins, BMCs more frequently appear as polyhedra, rather than as icosahedra, are usually much larger (100–600 nm) (35–41), and all BMC shells are composed of multiple paralogous shell proteins. A survey of all functionally diverse BMC loci in genomic sequence data showed that, on average, shell chromosomal loci encode 1.7 BMC-P, 2.6 BMC-H, and 1.2 BMC-T proteins (10). This likely reflects a key functional attribute of BMC shells: selective permeability for the substrates and products of the encapsulated enzymatic reactions. This multiplicity, and that the composition of the shell may be responsive to environmental conditions, may contribute to the observed pleiomorphy of native BMCs (Fig. 3). However, when most BMC shell proteins are expressed or assembled together *in vitro*, in the absence of their protein cargo, they typically form regular icosahedra that are very homogeneous (Fig. 3) (42–47), structurally analogous to viruses. However, there are some exceptions to this rule (48, 49); this point will be discussed more in-depth in later sections.

Assembly pathways: commonalities and deviations among shells

Smaller T number shells (ranging in complexity from T=1 to T=52 for viruses), encapsulins (T=1 to T=4), and empty BMC shells (T=4 to T=9) follow traditional groupings of hexons and pentons observed in classically described icosahedra (50). These organizations start to shift at larger sizes in viruses (e.g., giant viruses; T=>100), as they take on a different global organization formed from larger aggregates called pentasymmetrons and trisymmetrons (51). No such aggregate basic units are known for empty BMC shells or native BMCs (i.e., composed of protein cargo and shell).

While smaller T number icosahedral viruses all form from the same organization of hexon and penton building blocks, there is a distinct deviation in the order of assembly.

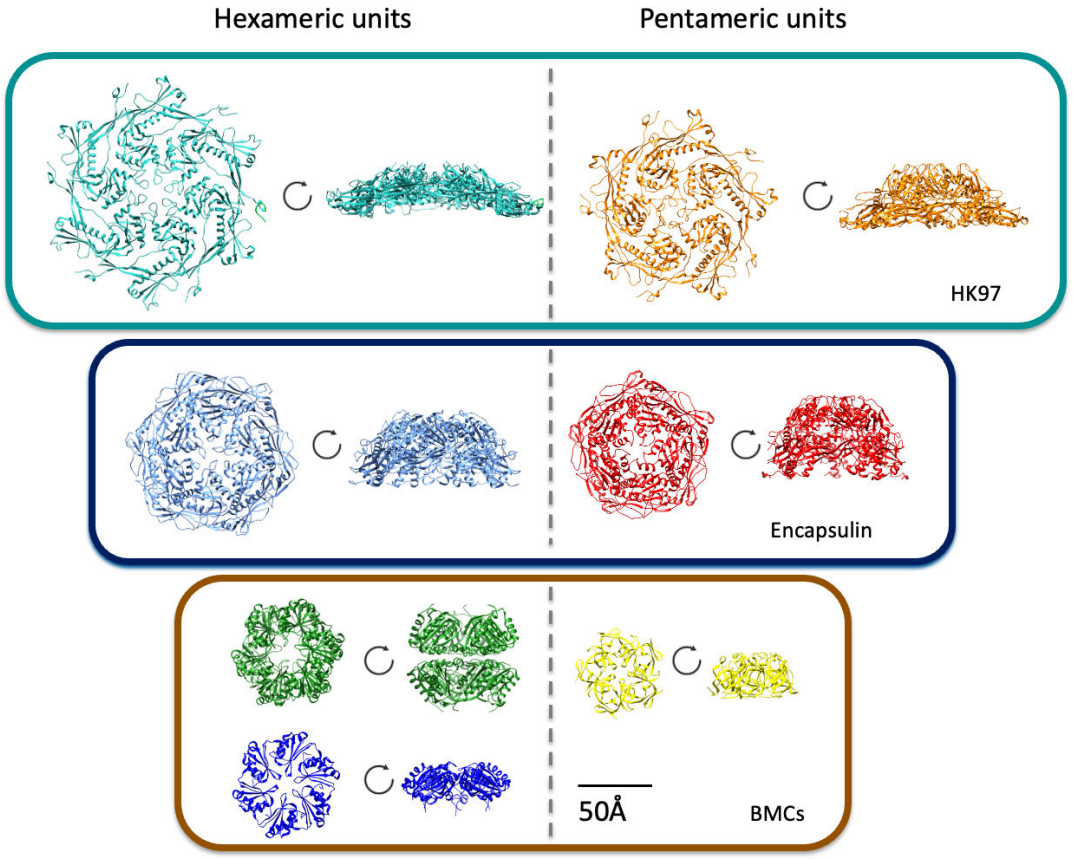

FIG 2 Tile subunits for viruses, encapsulins, and BMCs: Hexameric and pentameric grouping for HK97 (PDB 1OHG), *Myxococcus xanthus* EncA (PDB 8VJO), and *Haliangium ochraceum* microcompartment shells (PDB 5V74). Note, there are two types of hexameric building blocks for microcompartment shells: BMC-T (green) and BMC-H (blue). Top-down and side views are shown. All images are at the same scale (50 Å).

Many icosahedral viruses typically assemble from a penton first. Rules governing icosahedral virus assembly have been derived from a number of well-studied groups. First, some viral capsids are formed exclusively from pentons, such as T=1 capsids, including animal viruses such as parvoviruses (52), fungal viruses, and plant viruses (53, 54). These penton-only structures suggest hexons are dispensable for initiating assembly. Additionally, the T=7 polyoma virus assembles from 72 pentameric subunits (55), indicating hexons are not necessarily needed to form larger, more complex icosahedra. Other evidence suggests that a wide array of viruses assemble first from pentameric vertices such as most, if not all, dsDNA phage and some eukaryotic viruses (herpes and adenovirus), ssDNA phage, and giant viruses (56–58). In many cases, this may result from the requirement of breaking strict icosahedral symmetry at a single unique vertex that can accommodate a portal or a stargate for dsDNA packaging and egress, and may also serve as the site of tail or tube attachment (59). However, not all icosahedral viruses begin assembly at a five-fold axis of symmetry. For example, phage MS2 assembly is proposed to initiate at a threefold symmetry site (60).

Interestingly, the penton-hexon interface can be a weak point in icosahedral shells. For phage P22, heat stress can cause the pentons to release (61, 62). Atomic force microscopy studies also show mechanical failure for herpesviruses is localized to the pentons as well (63). For empty BMC shells, incomplete occupancy of pentamers is well documented. This was first observed during the structure determination of an empty metabolosome shell. Crystals of 6.5 MDa empty recombinant BMC shell initially diffracted poorly. Expression of additional copies of the pentamer improved diffraction to 3.5 Å (43), leading to a model containing all of the distinct subunit interactions within an empty, icosahedral BMC shell. For native BMCs, fluorescence-based imaging methods

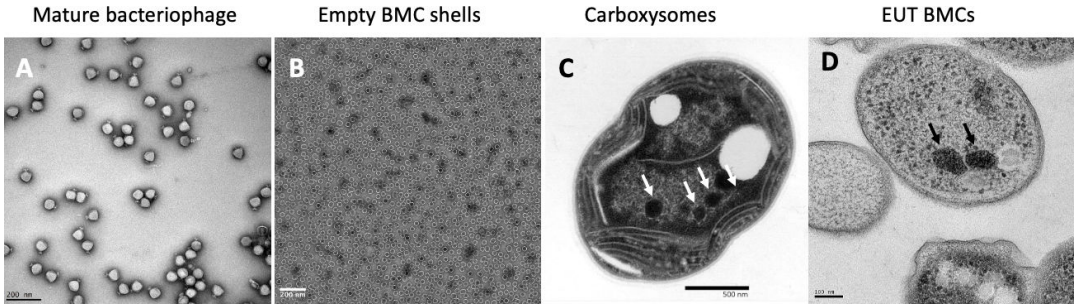

FIG 3 Bacteriophage, BMCs, and carboxysome morphologies: *in vivo* assembled particles. (A) A representative micrograph of negatively stained short-tailed podophage CUS-3. Image by Kristin Parent. (B) Negatively stained empty BMC shells produced by heterologous expression of *Haliangium ochraceum* shell proteins. Image courtesy of Tim Chiang, reproduced with permission. (C) Negatively stained thin section micrograph showing cyanobacterial carboxysomes. Image courtesy of Sarah Pacheco, reproduced with permission. (D) Negatively stained thin section micrograph showing EUT BMCs. Image courtesy of Doug Huseby, Rick Webb, and Cheryl Kerfeld, reproduced with permission.

for inventorying the components of the beta carboxysome indicate that pentamers are present in substoichiometric amounts (64, 65). This has been suggested to reflect dynamics of pentamer association/dissociation in native BMCs, which could allow for enzymatic core remodeling and repair and is proposed as a factor in the observed morphological heterogeneity (64, 65). Currently, little is known about the assembly pathway for empty BMC shells, but what we do know suggests it is likely not driven by pentamer-first kinetics, as pentons can be absent.

In vivo assembly pathways among biological shells and departures from icosahedral symmetry

Initiation of assembly differs among naturally occurring biological polyhedra. Some viral capsids, such as all dsDNA-containing tailed bacteriophages and herpesviruses, assemble first into precursor structures called procapsids from interactions between the major capsid protein and the scaffolding proteins, which are largely helical proteins that assemble the major coat protein subunits via electrostatic interactions (66–74). Scaffolding proteins then either leave the shells intact (e.g., phage P22) or are cleaved (e.g., herpesviruses), and the peptide byproducts leave via pores in the hexons. A maturation event then typically occurs that results in expansion of the head volume to accommodate packaging of the genome by ATP-driven motors, most often terminases (18), but other motor types are observed as well, such as in phi29 (75). Similar morphogenesis pathways likely occur for some giant viruses that also contain portal complexes and active ATPase packaging proteins (76).

In addition to the highly specific interactions between scaffolding proteins and the major coat proteins, some viruses also selectively package other phage-encoded proteins that remain inside the viral shell during maturation. Some examples are the so-called "E-proteins," or ejection proteins in phages P22 (77), DEV (78), and the H protein in phiX174 (79). These encapsidated proteins are used during the infection step; they are jettisoned from inside the capsid to form a tubular structure that helps transfer the genome from the phage across the host cell membrane into the cytoplasm. Another example of selectively packaged proteins in viral capsids includes virally encoded polymerases such as seen in phage N4 (80) as well as Hepatitis B Virus (81), rotaviruses (82), and reoviruses (83). Lastly, some Mimivirus-like giant viruses selectively package a large number of different proteins (~50–80 distinct proteins) into an extra membrane sac which is encapsidated in the virion, and is also likely used during the initial stages of infection (84). Alternatively, many icosahedral viruses can assemble directly around their genomes, especially viruses with single-stranded genomes (85), for example, ssRNA phages like MS2 (60), plant viruses such as CCMV (86), or animal viruses such as picornoviruses (87, 88). Regardless of whether it is scaffolding protein-mediated

or genome-mediated assembly, the end state for all known mature virions is that the majority of packaged cargo is genetic material, be it RNA, DNA, or a mixture of both, with a minority of the cargo (34) including proteins.

In addition to classical wet lab experimentation, computational approaches are also being applied to study assembly of isometric viral shells (89, 90), as well as less regularly shaped (e.g., human immunodeficiency virus [91] and others [92]), and much larger polyhedra (e.g., giant viruses [93]). The following is a brief summation of the general principles learned that govern icosahedral assembly for a variety of examples. Assembly of icosahedral cages can either be by (i) the addition of monomeric subunits, one at a time (e.g., phage P22 [94]), (ii) by preformed tiles already assembled into hexon and penton organizations (e.g., phage HK97 [95]), or (iii) in smaller viruses, assembly can be observed from dimers as in hepatitis B virus (HBV) (96). Both traditional experimentation and computational approaches converge to similar themes: these assembly pathways are generally high fidelity and occur on similar kinetic time scales (85, 97). Time scales of assembly are linked tightly to the biology. As one example, for bacteriophages, assembly occurs within minutes at biological temperatures as the doubling time of the host is usually on the order of 20–30 minutes. Similarly, assembly of encapsulins is observed to take ~15–30 minutes *in vitro* (98). However, our understanding of the influence of kinetics on capsid assembly is not yet complete. Kinetic traps can form if assembly rates, especially involving nucleation, are too high, as too many starting places form and free subunits become rapidly depleted (99), resulting in incomplete particles. By contrast, a more recent study suggested that faster assembly times are beneficial, as they can lead to fewer aberrant particles by skipping over highly stable pentameric kinetic traps, as shown with human papillomavirus (HPV) (100). Assembly environment matters: coarse-grained molecular dynamics simulations show that biomolecular condensates can enhance assembly rates and robustness, and this might explain the importance of viral factories (101). Perhaps if slow and "correct" nucleation is achieved, coupled with faster elongation, kinetics can improve viral capsid yields.

Once formed, viral icosahedral shells tend to be highly stable. And from an assembly perspective, relatively weak protein:protein interactions build to form very stable icosahedra products (102, 103). Yet, dissociation of viral subunits can also be observed on experimental time scales, indicating these are not inert, irreversible assemblies (104, 105). In addition, many viruses need to dissociate or disrupt their icosahedral capsids *in vivo* as part of the natural infection processes. Often, overcoming this thermodynamic barrier to disrupting the icosahedral shell requires perturbation. Some examples can be from interactions with cellular factors, such as receptor proteins (106), interactions with the nuclear pore complex (107), changes in pH (84), and others, as well as interactions with abiotic factors, such as binding to drug molecules (108), etc. Disassembly pathways have been notoriously difficult to study experimentally; this is an emerging area for computational approaches such as molecular dynamics (109).

In contrast, encapsulins and BMCs exclusively compartmentalize proteinaceous cargo, rather than nucleic acids. BMCs are metabolically diverse—there are over 60 functionally distinct types encapsulating a diverse array of enzymes and type-specific scaffolding proteins (10, 110). Encapsulins, on the other hand, are more limited in the types and amounts of cargo they encapsulate via targeting domains/peptides (28, 31, 111). Encapsulin assembly is more similar to virus assembly than to BMC assembly. Phage and encapsulin building blocks have homologous folds (Fig. 1). The assembly process of encapsulins is also highly specific. It is usually driven by the products of a two-gene system, including a shell protein and a cargo protein. Encapsulin assembly pathways can occur via one of two "modes." Either C-terminal peptides drive specific cargo encapsulation, or N-terminal domains regulate assembly (112, 113). Recent work using cryo-EM studies has revealed encapsulin assembly intermediates both *in vivo* and *in vitro* and suggests assembly is driven by pairwise addition of monomers (114).

Unlike both viruses and encapsulins, departure from strict icosahedral symmetry is the rule, not the exception, for native BMC systems (Fig. 3) (35–41). Furthermore,

despite their structurally analogous shell protein building blocks with their potential to self-assemble into icosahedra (Fig. 2), unlike viruses, assembly of BMCs is strongly influenced by cargo. Theoretical studies have underscored the important role of the encapsulated proteins in dictating BMC size and morphology (115–118) through both kinetic and thermodynamic influences.

Given the observed heterogeneity of BMC polyhedra in cells (Fig. 3), diverse pathways for their assembly are expected. In the first BMC assembly pathway to be experimentally deduced, for the beta carboxysome (Fig. 3C), nucleation of the enzymatic core is the initial step, followed by incorporation of the shell. In this BMC, the central cargo enzyme ribulose-1,5-bisphosphate carboxylase/oxygenase (RuBisCo) is composed of eight small (RbcS) and eight large (RbcL) subunits. It is packaged with a gamma carbonic anhydrase, CcmM, which, in addition to its carbonic anhydrase domain, contains multiple copies of RbcS-like domains, which provide interaction sites with RuBisCo. A third protein, CcmN, contains gamma carbonic anhydrase-like repeats, a variable length, poorly conserved, disordered linker region, and a C-terminal encapsulation peptide (119), shown to interact with the carboxysome shell proteins (115). This type of assembly pathway, involving both enzymes and proteins with domains or regions that mimic the enzyme components to function in scaffolding (115, 117), is likely to be widespread among functionally diverse BMCs. Domain mimics are known in several BMC types (10, 120), and encapsulation peptides are found in the majority of BMCs (119, 121). Indeed, encapsulation peptides have long been known to cause aggregation of BMC enzymes (122–124) and now are emerging as part of a general strategy for biomolecular condensation with applications in biotechnology (125).

In contrast, the alpha carboxysome, which is evolutionarily distinct from the beta carboxysome (126), appears to have distinct assembly modes; both potential for a "shell-first" pathway (127) or concomitant assembly of shell and core proteins (128, 129). Notably, the morphology and size of alpha carboxysomes tend to be more regular and more frequently icosahedral; this may be related to more complete capping of the vertices by the BMC-P paralogs (130). Similar flexibility in the assembly modes of the propanediol metabolosome (PDU BMCs) was recently described (131), as well as the observation that specific extensions of some shell proteins play a role in the interactions between shell and cargo (131, 132). Likewise, similar to the beta carboxysome and other characterized BMC cores (133, 134), cargo enzymes form complexes that likely enhance catalytic efficiency. Assembly of the ethanolamine ("EUT") metabolosome (Fig. 3B) provides a third variation among BMC assembly themes; it is initiated by shell formation; however, distinct aggregates of both the shell and the core enzymes can form as stages in assembly (135).

Convergences of capsids and BMC shells in pleiomorphic space

Although relatively less frequently observed, viral capsids departing from symmetric icosahedral symmetry can occur by a number of means and still result in the formation of functional shells. Some examples include altered distribution of pentamers. For example, cones of various sizes and overall morphology can be seen in human immunodeficiency virus, HIV-1 by cryo-electron tomography (136). Interestingly, an empty BMC shell with a similar nanocone morphology is found among icosahedral shells and nanotubes formed by heterologous expression of the six distinct shell proteins (4 BMC-H, 1 BMC-T, and 1 BMC-P) from a purple bacterial BMC (49). In addition, partially capped "whiffle ball" BMC shells can form, and these demonstrate increased permeability relative to fully capped shells (137). Some natural BMC systems, such as glycyl radical enzyme-associated microcompartments ("GRM"), have enormous shape variation (36), and others like HO are more uniform. It is unknown yet whether or not the polyhedral shape of *in vivo* assembled shells is critical for their function. However, observational studies show that in HO shells, the less uniform shells (*in vivo*-assembled) have similar catalytic activity of packaged cargo compared with the *in vitro* assembled shells (138). Combined, these data

suggest uniform morphology shells may be fully functional, and that polyhedral variance is likely not by design or necessity.

In viruses, off-pathway assemblies can also occur that drive the formation of non-functional forms. Phage MS2 can naturally assemble into a mixture of forms, including functional particles as well as oblong shapes, both *in silico* (139) and *in vivo* (140), by altered interactions with the RNA genome. Mixed populations of icosahedra containing smaller or larger triangulation numbers can occur natively such as the presence of both T=3 and T=4 particles in hepatitis B virus infections (141, 142). Deviations in terms of frequency of "incorrectly" shaped or sized viral particles within populations can arise due to mutations or deletions in genes of regulating proteins, such as scaffolding proteins. Both mutations and deletions can give rise to altered virion types at an increased frequency compared to native infections. Commonly observed off-pathway assemblies have been studied extensively in bacteriophage P22. For example, deletion of scaffolding protein results in both T=7 native particles, as well as smaller T=4 particles (143). Mutations in either the coat protein (144) or deletions in the scaffolding protein (145) can also give rise to "spirals," where the pentons are located inappropriately, and the shells are unable to form completely closed icosahedra. In addition, mutations can also cause non-functional particle types such as sheets and tubes, which can form from relatively conservative, single amino acid capsid protein substitutions (144, 146, 147). For BMC systems, sheets and tubes are readily assembled by diverse shell proteins when assembled without cargo and out of their native context (42–45, 47, 49, 148–153).

SUMMARY

Why is the icosahedron so prevalent in nature? Evolutionarily very diverse protein folds (Fig. 1) seem to converge to self-assemble into the same structure (icosahedron) for two main reasons: stability and efficiency. An icosahedron requires a limited number of genes and protein building blocks.

For viruses, smaller capsids hold tiny genomes, and the same capsid geometry can expand to accommodate a massive amount of genetic material—up to 2.5 Mbp for giant viruses. Pentons are needed to provide the curvature to preferentially form a sphere over a tube and to complete the shells, but wiffle balls (viral shells without pentons) are stable too. There are a limited number of polyhedra formed from identical building blocks (cube, tetrahedron, and octahedron) that are scalable (icosahedral and dodecahedral). Icosahedral structures are ideally suited for biological assemblies given their increased rotational symmetry over other forms, and this optimizes internal volumes needed for genome packaging efficiency, particularly important for larger T number viruses (154). BMC shell proteins in the absence of their cargo readily assemble into icosahedra but are more commonly polyhedral in their native context. In bacteria, BMC shells function in concert with the requirements of the encapsulated enzymes; the shells not only protect the enzymes but also serve as conduits for their substrates and products. The multiplicity of enzymes and the structural redundancy arising from the use of paralogous hexagonal tiles (BMC-H and BMC-T proteins) and pentagonal tiles (BMC-P) are likely related to the frequent observations of various sizes and polyhedral morphologies of BMCs in cells. Despite being composed of structurally analogous building blocks, cargo-dictated function of viral capsids and BMC shells likely underlies their contrasting adherence to and departure from strict icosahedral form.

ACKNOWLEDGMENTS

This work was supported as part of the Center for Catalysis in Biomimetic Confinement (CCBC), an Energy Frontier Research Center (EFRC) funded by the U.S. Department of Energy, Office of Science, Basic Energy Sciences under Award Number DE-SC0023395 to C.A.K., as well as the National Institutes of Health GM110185 and GM140803 to K.N.P.

We also thank Drs. Carolyn Teschke, Michaela TerAvest, and Megan Cross for their critical reading of the manuscript and helpful insights. Lastly, we thank Mr. Robert Houston for his help in finding references.

AUTHOR AFFILIATIONS

[1]Department of Biochemistry and Molecular Biology, Michigan State University, East Lansing, Michigan, USA
[2]Environmental Genomics and Systems Biology Division, Lawrence Berkeley National Laboratory, Berkeley, California, USA
[3]MSU-DOE Plant Research Laboratory, Michigan State University, East Lansing, Michigan, USA
[4]Molecular Biophysics and Integrated Bioimaging Division, Lawrence Berkeley National Laboratory, Berkeley, California, USA

AUTHOR ORCIDs

Kristin N. Parent http://orcid.org/0000-0002-6095-0628
Cheryl A. Kerfeld http://orcid.org/0000-0002-9977-8482

FUNDING

Funder	Grant(s)	Author(s)
U.S. Department of Energy	DE-SC0023395	Kristin N. Parent
National Institutes of Health	GM110185	Kristin N. Parent
National Institutes of Health	GM140803	Kristin N. Parent

AUTHOR CONTRIBUTIONS

Kristin N. Parent, Conceptualization, Formal analysis, Writing – original draft | Cheryl A. Kerfeld, Conceptualization, Formal analysis, Funding acquisition, Writing – review and editing

REFERENCES

1. Chung YH, Cai H, Steinmetz NF. 2020. Viral nanoparticles for drug delivery, imaging, immunotherapy, and theranostic applications. Adv Drug Deliv Rev 156:214–235. https://doi.org/10.1016/j.addr.2020.06.024
2. Selivanovitch E, Douglas T. 2019. Virus capsid assembly across different length scales inspire the development of virus-based biomaterials. Curr Opin Virol 36:38–46. https://doi.org/10.1016/j.coviro.2019.02.010
3. Nichols RJ, Cassidy-Amstutz C, Chaijarasphong T, Savage DF. 2017. Encapsulins: molecular biology of the shell. Crit Rev Biochem Mol Biol 52:583–594. https://doi.org/10.1080/10409238.2017.1337709
4. Giessen TW. 2016. Encapsulins: microbial nanocompartments with applications in biomedicine, nanobiotechnology and materials science. Curr Opin Chem Biol 34:1–10. https://doi.org/10.1016/j.cbpa.2016.05.013
5. Doron L, Kerfeld CA. 2024. Bacterial microcompartments as a next-generation metabolic engineering tool: utilizing nature's solution for confining challenging catabolic pathways. Biochem Soc Trans 52:997–1010. https://doi.org/10.1042/BST20230229
6. Kwon S, Giessen TW. 2025. Engineering encapsulin nanocages for drug delivery. Mater Adv 6:6209–6220. https://doi.org/10.1039/d5ma00386e
7. Caspar DLD, Klug A. 1962. Physical principles in the construction of regular viruses. Cold Spring Harb Symp Quant Biol 27:1–24. https://doi.org/10.1101/SQB.1962.027.001.005
8. Twarock R, Luque A. 2019. Structural puzzles in virology solved with an overarching icosahedral design principle. Nat Commun 10:4414. https://doi.org/10.1038/s41467-019-12367-3
9. Kerfeld CA, Aussignargues C, Zarzycki J, Cai F, Sutter M. 2018. Bacterial microcompartments. Nat Rev Microbiol 16:277–290. https://doi.org/10.1038/nrmicro.2018.10
10. Sutter M, Melnicki MR, Schulz F, Woyke T, Kerfeld CA. 2021. A catalog of the diversity and ubiquity of bacterial microcompartments. Nat Commun 12:3809. https://doi.org/10.1038/s41467-021-24126-4
11. Wikoff WR, Duda RL, Hendrix RW, Johnson JE. 1999. Crystallographic analysis of the dsDNA bacteriophage HK97 mature empty capsid. Acta Crystallogr D Biol Crystallogr 55:763–771. https://doi.org/10.1107/s0907444998017661
12. Wikoff WR, Liljas L, Duda RL, Tsuruta H, Hendrix RW, Johnson JE. 2000. Topologically linked protein rings in the bacteriophage HK97 capsid. Science 289:2129–2133. https://doi.org/10.1126/science.289.5487.2129
13. Bamford DH, Grimes JM, Stuart DI. 2005. What does structure tell us about virus evolution? Curr Opin Struct Biol 15:655–663. https://doi.org/10.1016/j.sbi.2005.10.012
14. Abrescia NGA, Bamford DH, Grimes JM, Stuart DI. 2012. Structure unifies the viral universe. Annu Rev Biochem 81:795–822. https://doi.org/10.1146/annurev-biochem-060910-095130
15. Stehle T, Gamblin SJ, Yan Y, Harrison SC. 1996. The structure of simian virus 40 refined at 3.1 A resolution. Structure 4:165–182. https://doi.org/10.1016/s0969-2126(96)00020-2
16. López-Bueno A, Gil-Ranedo J, Almendral JM. 2024. Assembly of structurally simple icosahedral viruses. Subcell Biochem 105:403–430. https://doi.org/10.1007/978-3-031-65187-8_11
17. Stivala A, Wybrow M, Wirth A, Whisstock JC, Stuckey PJ. 2011. Automatic generation of protein structure cartoons with Pro-origami. Bioinformatics 27:3315–3316. https://doi.org/10.1093/bioinformatics/btr575
18. Teschke CM, Parent KN. 2010. "Let the phage do the work": using the phage P22 coat protein structures as a framework to understand its folding and assembly mutants. Virology (Auckl) 401:119–130. https://doi.org/10.1016/j.virol.2010.02.017

19. Suhanovsky MM, Teschke CM. 2015. Nature's favorite building block: deciphering folding and capsid assembly of proteins with the HK97-fold. Virology (Auckl) 479–480:487–497. https://doi.org/10.1016/j.virol.2015.02.055
20. Fokine A, Chipman PR, Leiman PG, Mesyanzhinov VV, Rao VB, Rossmann MG. 2004. Molecular architecture of the prolate head of bacteriophage T4. Proc Natl Acad Sci USA 101:6003–6008. https://doi.org/10.1073/pnas.0400444101
21. Chen Z, Sun L, Zhang Z, Fokine A, Padilla-Sanchez V, Hanein D, Jiang W, Rossmann MG, Rao VB. 2017. Cryo-EM structure of the bacteriophage T4 isometric head at 3.3-Å resolution and its relevance to the assembly of icosahedral viruses. Proc Natl Acad Sci USA 114:E8184–E8193. https://doi.org/10.1073/pnas.1708483114
22. Jacobson MF, Baltimore D. 1968. Polypeptide cleavages in the formation of poliovirus proteins. Proc Natl Acad Sci USA 61:77–84. https://doi.org/10.1073/pnas.61.1.77
23. Basavappa R, Syed R, Flore O, Icenogle JP, Filman DJ, Hogle JM. 1994. Role and mechanism of the maturation cleavage of VP0 in poliovirus assembly: structure of the empty capsid assembly intermediate at 2.9 A resolution. Protein Sci 3:1651–1669. https://doi.org/10.1002/pro.5560031005
24. Srivastava A, Lusby EW, Berns KI. 1983. Nucleotide sequence and organization of the adeno-associated virus 2 genome. J Virol 45:555–564. https://doi.org/10.1128/JVI.45.2.555-564.1983
25. DeCaprio JA, Garcea RL. 2013. A cornucopia of human polyomaviruses. Nat Rev Microbiol 11:264–276. https://doi.org/10.1038/nrmicro2992
26. Duda RL, Teschke CM. 2019. The amazing HK97 fold: versatile results of modest differences. Curr Opin Virol 36:9–16. https://doi.org/10.1016/j.coviro.2019.02.001
27. Podgorski JM, Freeman K, Gosselin S, Huet A, Conway JF, Bird M, Grecco J, Patel S, Jacobs-Sera D, Hatfull G, Gogarten JP, Ravantti J, White SJ. 2023. A structural dendrogram of the actinobacteriophage major capsid proteins provides important structural insights into the evolution of capsid stability. Structure 31:282–294. https://doi.org/10.1016/j.str.2022.12.012
28. Giessen TW. 2022. Encapsulins. Annu Rev Biochem 91:353–380. https://doi.org/10.1146/annurev-biochem-040320-102858
29. Fontana J, Nemecek D, McHugh CA, Aksyuk AA, Cheng N, Winkler DC, Bernard Heymann J, Hoiczyk E, Steven AC. 2014. Phage capsid-like structure of *Myxococcus xanthus* encapsulin, a protein shell that stores iron. Microsc Microanal 20:1244–1245. https://doi.org/10.1017/S1431927614007958
30. Ubilla-Rodriguez NC, Andreas MP, Giessen TW. 2025. Structural and biochemical characterization of a widespread enterobacterial peroxidase encapsulin. Adv Sci (Weinh) 12:e2415827. https://doi.org/10.1002/advs.202415827
31. Jones JA, Benisch R, Giessen TW. 2023. Encapsulin cargo loading: progress and potential. J Mater Chem B 11:4377–4388. https://doi.org/10.1039/d3tb00288h
32. Andreas MP, Giessen TW. 2021. Large-scale computational discovery and analysis of virus-derived microbial nanocompartments. Nat Commun 12:4748. https://doi.org/10.1038/s41467-021-25071-y
33. Aguilar A, Miranda I, Nadel O, Nayfach S, Ruiz Pestana L, Segall AM, Rohwer FL, Roux S, White S, Luque A. 2025. Small viruses reveal bidirectional evolution between HK97-fold viruses and encapsulins via procapsids. bioRxiv. https://doi.org/10.1101/2025.06.18.659913:2025.06.18.659913
34. Kwon S, Andreas MP, Giessen TW. 2023. Structure and heterogeneity of a highly cargo-loaded encapsulin shell. J Struct Biol 215:108022. https://doi.org/10.1016/j.jsb.2023.108022
35. Petit E, LaTouf WG, Coppi MV, Warnick TA, Currie D, Romashko I, Deshpande S, Haas K, Alvelo-Maurosa JG, Wardman C, Schnell DJ, Leschine SB, Blanchard JL. 2013. Involvement of a bacterial microcompartment in the metabolism of fucose and rhamnose by *Clostridium phytofermentans*. PLoS One 8:e54337. https://doi.org/10.1371/journal.pone.0054337
36. Cesle EE, Filimonenko A, Tars K, Kalnins G. 2021. Variety of size and form of GRM2 bacterial microcompartment particles. Protein Sci 30:1035–1043. https://doi.org/10.1002/pro.4069
37. Herring TI, Harris TN, Chowdhury C, Mohanty SK, Bobik TA. 2018. A bacterial microcompartment is used for choline fermentation by *Escherichia coli* 536. J Bacteriol 200:e00764-17. https://doi.org/10.1128/JB.00764-17
38. Erbilgin O, McDonald KL, Kerfeld CA. 2014. Characterization of a planctomycetal organelle: a novel bacterial microcompartment for the aerobic degradation of plant saccharides. Appl Environ Microbiol 80:2193–2205. https://doi.org/10.1128/AEM.03887-13
39. Gonzalez-Esquer CR, Smarda J, Rippka R, Axen SD, Guglielmi G, Gugger M, Kerfeld CA. 2016. Cyanobacterial ultrastructure in light of genomic sequence data. Photosynth Res 129:147–157. https://doi.org/10.1007/s11120-016-0286-2
40. Kennedy NW, Hershewe JM, Nichols TM, Roth EW, Wilke CD, Mills CE, Jewett MC, Tullman-Ercek D. 2020. Apparent size and morphology of bacterial microcompartments varies with technique. PLoS One 15:e0226395. https://doi.org/10.1371/journal.pone.0226395
41. Mayer MJ, Juodeikis R, Brown IR, Frank S, Palmer DJ, Deery E, Beal DM, Xue WF, Warren MJ. 2016. Effect of bio-engineering on size, shape, composition and rigidity of bacterial microcompartments. Sci Rep 6:36899. https://doi.org/10.1038/srep36899
42. Sutter M, Laughlin TG, Sloan NB, Serwas D, Davies KM, Kerfeld CA. 2019. Structure of a synthetic beta-carboxysome shell. Plant Physiol 181:1050–1058. https://doi.org/10.1104/pp.19.00885
43. Sutter M, Greber B, Aussignargues C, Kerfeld CA. 2017. Assembly principles and structure of a 6.5-MDa bacterial microcompartment shell. Science 356:1293–1297. https://doi.org/10.1126/science.aan3289
44. Cai F, Bernstein SL, Wilson SC, Kerfeld CA. 2016. Production and characterization of synthetic carboxysome shells with incorporated luminal proteins. Plant Physiol 170:1868–1877. https://doi.org/10.1104/pp.15.01822
45. Lassila JK, Bernstein SL, Kinney JN, Axen SD, Kerfeld CA. 2014. Assembly of robust bacterial microcompartment shells using building blocks from an organelle of unknown function. J Mol Biol 426:2217–2228. https://doi.org/10.1016/j.jmb.2014.02.025
46. Kalnins G, Cesle EE, Jansons J, Liepins J, Filimonenko A, Tars K. 2020. Encapsulation mechanisms and structural studies of GRM2 bacterial microcompartment particles. Nat Commun 11:388. https://doi.org/10.1038/s41467-019-14205-y
47. Li T, Chang P, Chen W, Shi Z, Xue C, Dykes GF, Huang F, Wang Q, Liu LN. 2024. Nanoengineering carboxysome shells for protein cages with programmable cargo targeting. ACS Nano 18:7473–7484. https://doi.org/10.1021/acsnano.3c11559
48. Trettel DS, Winkler WC. 2023. *In vitro* analysis of bacterial microcompartments and shell protein superstructures by confocal microscopy. Microbiol Spectr 11:e0335722. https://doi.org/10.1128/spectrum.03357-22
49. Ferlez BH, Kirst H, Greber BJ, Nogales E, Sutter M, Kerfeld CA. 2023. Heterologous assembly of pleomorphic bacterial microcompartment shell architectures spanning the nano- to microscale. Adv Mater Weinheim 35:e2212065. https://doi.org/10.1002/adma.202212065
50. Hua J, Huet A, Lopez CA, Toropova K, Pope WH, Duda RL, Hendrix RW, Conway JF. 2017. Capsids and genomes of jumbo-sized bacteriophages reveal the evolutionary reach of the HK97 fold. mBio 8. https://doi.org/10.1128/mBio.01579-17
51. Sinkovits RS, Baker TS. 2010. A tale of two symmetrons: rules for construction of icosahedral capsids from trisymmetrons and pentasymmetrons. J Struct Biol 170:109–116. https://doi.org/10.1016/j.jsb.2009.12.003
52. Mietzsch M, Pénzes JJ, Agbandje-McKenna M. 2019. Twenty-five years of structural parvovirology. Viruses 11:362. https://doi.org/10.3390/v11040362
53. Luque D, Mata CP, Suzuki N, Ghabrial SA, Castón JR. 2018. Capsid structure of dsRNA fungal viruses. Viruses 10:481. https://doi.org/10.3390/v10090481
54. Rossmann MG, Abad-Zapatero C, Erickson JW, Savithri HS. 1983. RNA-protein interactions in some small plant viruses. J Biomol Struct Dyn 1:565–579. https://doi.org/10.1080/07391102.1983.10507462
55. Salunke DM, Caspar DL, Garcea RL. 1986. Self-assembly of purified polyomavirus capsid protein VP1. Cell 46:895–904. https://doi.org/10.1016/0092-8674(86)90071-1
56. Dedeo CL, Cingolani G, Teschke CM. 2019. Portal protein: the orchestrator of capsid assembly for the dsDNA tailed bacteriophages and herpesviruses. Annu Rev Virol 6:141–160. https://doi.org/10.1146/annurev-virology-092818-015819
57. Doore SM, Fane BA. 2016. The microviridae: diversity, assembly, and experimental evolution. Virology (Auckl) 491:45–55. https://doi.org/10.1016/j.virol.2016.01.020

58. Xian Y, Xiao C. 2020. Current capsid assembly models of icosahedral nucleocytoviricota viruses. Adv Virus Res 108:275–313. https://doi.org/10.1016/bs.aivir.2020.09.006
59. Parent KN, Schrad JR, Cingolani G. 2018. Breaking symmetry in viral icosahedral capsids as seen through the lenses of X-ray crystallography and cryo-electron microscopy. Viruses 10:67. https://doi.org/10.3390/v10020067
60. Stockley PG, White SJ, Dykeman E, Manfield I, Rolfsson O, Patel N, Bingham R, Barker A, Wroblewski E, Chandler-Bostock R, Weiß EU, Ranson NA, Tuma R, Twarock R. 2016. Bacteriophage MS2 genomic RNA encodes an assembly instruction manual for its capsid. Bacteriophage 6:e1157666. https://doi.org/10.1080/21597081.2016.1157666
61. Parent KN, Khayat R, Tu LH, Suhanovsky MM, Cortines JR, Teschke CM, Johnson JE, Baker TS. 2010. P22 coat protein structures reveal a novel mechanism for capsid maturation: stability without auxiliary proteins or chemical crosslinks. Structure 18:390–401. https://doi.org/10.1016/j.str.2009.12.014
62. Teschke CM, McGough A, Thuman-Commike PA. 2003. Penton release from P22 heat-expanded capsids suggests importance of stabilizing penton-hexon interactions during capsid maturation. Biophys J 84:2585–2592. https://doi.org/10.1016/S0006-3495(03)75063-2
63. Roos WH, Gertsman I, May ER, Brooks CL III, Johnson JE, Wuite GJL. 2012. Mechanics of bacteriophage maturation. Proc Natl Acad Sci USA 109:2342–2347. https://doi.org/10.1073/pnas.1109590109
64. Sun Y, Sheng Y, Ni T, Ge X, Sarsby J, Brownridge PJ, Li K, Hardenbrook N, Dykes GF, Rockliffe N, Eyers CE, Zhang P, Liu L-N. 2024. Rubisco packaging and stoichiometric composition of the native β-carboxysome in *Synechococcus elongatus* PCC7942. Plant Physiol 197:kiae665. https://doi.org/10.1093/plphys/kiae665
65. Sun Y, Wollman AJM, Huang F, Leake MC, Liu LN. 2019. Single-organelle quantification reveals stoichiometric and structural variability of carboxysomes dependent on the environment. Plant Cell 31:1648–1664. https://doi.org/10.1105/tpc.18.00787
66. Bazinet C, King J. 1988. Initiation of P22 procapsid assembly *in vivo*. J Mol Biol 202:77–86. https://doi.org/10.1016/0022-2836(88)90520-7
67. Brown JC, Newcomb WW. 2011. Herpesvirus capsid assembly: insights from structural analysis. Curr Opin Virol 1:142–149. https://doi.org/10.1016/j.coviro.2011.06.003
68. Casjens S, King J. 1974. P22 morphogenesis. I: Catalytic scaffolding protein in capsid assembly. J Supramol Struct 2:202–224. https://doi.org/10.1002/jss.400020215
69. Choi KH, Morais MC, Anderson DL, Rossmann MG. 2006. Determinants of bacteriophage phi29 head morphology. Structure 14:1723–1727. https://doi.org/10.1016/j.str.2006.09.007
70. Dokland T. 1999. Scaffolding proteins and their role in viral assembly. Cell Mol Life Sci 56:580–603. https://doi.org/10.1007/s000180050455
71. Dokland T, Bernal RA, Burch A, Pletnev S, Fane BA, Rossmann MG. 1999. The role of scaffolding proteins in the assembly of the small, single-stranded DNA virus phiX174. J Mol Biol 288:595–608. https://doi.org/10.1006/jmbi.1999.2699
72. Leroux MN, Skidds GS, Teschke CM. 2025. Elucidating double stranded DNA viral scaffolding protein structures through advances in cryogenic electron microscopy data processing. Curr Opin Struct Biol 94:103081. https://doi.org/10.1016/j.sbi.2025.103081
73. Cortines JR, Motwani T, Vyas AA, Teschke CM. 2014. Highly specific salt bridges govern bacteriophage P22 icosahedral capsid assembly: identification of the site in coat protein responsible for interaction with scaffolding protein. J Virol 88:5287–5297. https://doi.org/10.1128/JVI.00036-14
74. Padilla-Meier GP, Gilcrease EB, Weigele PR, Cortines JR, Siegel M, Leavitt JC, Teschke CM, Casjens SR. 2012. Unraveling the role of the C-terminal helix turn helix of the coat-binding domain of bacteriophage P22 scaffolding protein. J Biol Chem 287:33766–33780. https://doi.org/10.1074/jbc.M112.393132
75. Jardine PJ. 2019. Slow and steady wins the race: physical limits on the rate of viral DNA packaging. Curr Opin Virol 36:32–37. https://doi.org/10.1016/j.coviro.2019.03.002
76. Talbert PB, Henikoff S, Armache KJ. 2023. Giant variations in giant virus genome packaging. Trends Biochem Sci 48:1071–1082. https://doi.org/10.1016/j.tibs.2023.09.003
77. Israel V. 1977. E proteins of bacteriophage P22. I. Identification and ejection from wild-type and defective particles. J Virol 23:91–97. https://doi.org/10.1128/JVI.23.1.91-97.1977
78. Lokareddy RK, Hou C-F, Forti F, Iglesias SM, Li F, Pavlenok M, Horner DS, Niederweis M, Briani F, Cingolani G. 2024. Integrative structural analysis of *Pseudomonas* phage DEV reveals a genome ejection motor. Nat Commun 15:8482. https://doi.org/10.1038/s41467-024-52752-1
79. Sun L, Rossmann MG, Fane BA. 2014. High-resolution structure of a virally encoded DNA-translocating conduit and the mechanism of DNA penetration. J Virol 88:10276–10279. https://doi.org/10.1128/JVI.00291-14
80. Falco SC, Laan KV, Rothman-Denes LB. 1977. Virion-associated RNA polymerase required for bacteriophage N4 development. Proc Natl Acad Sci USA 74:520–523. https://doi.org/10.1073/pnas.74.2.520
81. Bartenschlager R, Schaller H. 1992. Hepadnaviral assembly is initiated by polymerase binding to the encapsidation signal in the viral RNA genome. EMBO J 11:3413–3420. https://doi.org/10.1002/j.1460-2075.1992.tb05420.x
82. Gridley CL, Patton JT. 2014. Regulation of rotavirus polymerase activity by inner capsid proteins. Curr Opin Virol 9:31–38. https://doi.org/10.1016/j.coviro.2014.08.008
83. Liu H, Cheng L. 2022. Viral capsid and polymerase in reoviridae, p 525–552. In Macromolecular protein complexes IV: structure and function. Springer International Publishing, Cham.
84. Schrad JR, Abrahão JS, Cortines JR, Parent KN. 2020. Structural and proteomic characterization of the initiation of giant virus infection. Cell 181:1046–1061. https://doi.org/10.1016/j.cell.2020.04.032
85. Perlmutter JD, Hagan MF. 2015. Mechanisms of virus assembly. Annu Rev Phys Chem 66:217–239. https://doi.org/10.1146/annurev-physchem-040214-121637
86. Garmann RF, Comas-Garcia M, Koay MST, Cornelissen J, Knobler CM, Gelbart WM. 2014. Role of electrostatics in the assembly pathway of a single-stranded RNA virus. J Virol 88:10472–10479. https://doi.org/10.1128/JVI.01044-14
87. Nugent CI, Kirkegaard K. 1995. RNA binding properties of poliovirus subviral particles. J Virol 69:13–22. https://doi.org/10.1128/JVI.69.1.13-22.1995
88. Gil-Cantero D, Mata CP, Valiente L, Rodríguez-Huete A, Valbuena A, Twarock R, Stockley PG, Mateu MG, Castón JR. 2024. Cryo-EM of human rhinovirus reveals capsid-RNA duplex interactions that provide insights into virus assembly and genome uncoating. Commun Biol 7:1501. https://doi.org/10.1038/s42003-024-07213-2
89. Li S, Tresset G, Zandi R. 2025. From disorder to icosahedral symmetry: How conformation-switching subunits enable RNA virus assembly. Sci Adv 11:eady7241. https://doi.org/10.1126/sciadv.ady7241
90. Frechette LB, Sundararajan N, Caballero F, Trubiano A, Hagan MF. 2025. Computer simulations show that liquid-liquid phase separation enhances self-assembly. ACS Nano 19:30275–30291. https://doi.org/10.1021/acsnano.5c08120
91. Zhao G, Perilla JR, Yufenyuy EL, Meng X, Chen B, Ning J, Ahn J, Gronenborn AM, Schulten K, Aiken C, Zhang P. 2013. Mature HIV-1 capsid structure by cryo-electron microscopy and all-atom molecular dynamics. Nature 497:643–646. https://doi.org/10.1038/nature12162
92. Pérez-Segura C, Perilla JR, Hadden-Perilla JA. 2025. Atomistic simulations of intact virus capsids: a computational challenge worth the scientific payoff. Curr Opin Struct Biol 93:103082. https://doi.org/10.1016/j.sbi.2025.103082
93. Xian Y, Karki CB, Silva SM, Li L, Xiao C. 2019. The roles of electrostatic interactions in capsid assembly mechanisms of giant viruses. Int J Mol Sci 20:1876. https://doi.org/10.3390/ijms20081876
94. Teschke CM, King J. 1993. Folding of the phage P22 coat protein *in vitro*. Biochemistry 32:10839–10847. https://doi.org/10.1021/bi00091a040
95. Xie Z, Hendrix RW. 1995. Assembly *in vitro* of bacteriophage HK97 proheads. J Mol Biol 253:74–85. https://doi.org/10.1006/jmbi.1995.0537
96. Buzón P, Maity S, Christodoulis P, Wiertsema MJ, Dunkelbarger S, Kim C, Wuite GJL, Zlotnick A, Roos WH. 2021. Virus self-assembly proceeds through contact-rich energy minima. Sci Adv 7:eabg0811. https://doi.org/10.1126/sciadv.abg0811
97. Singh S, Zlotnick A. 2003. Observed hysteresis of virus capsid disassembly is implicit in kinetic models of assembly. J Biol Chem 278:18249–18255. https://doi.org/10.1074/jbc.M211408200
98. Boyton I, Goodchild SC, Diaz D, Elbourne A, Collins-Praino LE, Care A. 2022. Characterizing the dynamic disassembly/reassembly mechanisms of encapsulin protein nanocages. ACS Omega 7:823–836. https://doi.org/10.1021/acsomega.1c05472
99. Parent KN, Doyle SM, Anderson E, Teschke CM. 2005. Electrostatic interactions govern both nucleation and elongation during phage P22

procapsid assembly. Virology (Auckl) 340:33–45. https://doi.org/10.1016/j.virol.2005.06.018
100. Klein SM, Patterson A, Young K, Biever MP, Miller LM, Zlotnick A, Jacobson SC, Jarrold MF. 2025. Speed matters: directed assembly of icosahedral HPV virus-like particles. J Am Chem Soc 147:24950–24957. https://doi.org/10.1021/jacs.5c07472
101. Frechette LB, Sundararajan N, Caballero F, Trubiano A, Hagan MF. 2025. Computer simulations show that liquid–liquid phase separation enhances self-assembly. ACS Nano 19:30275–30291. https://doi.org/10.1021/acsnano.5c08120
102. Katen S, Zlotnick A. 2009. The thermodynamics of virus capsid assembly. Methods Enzymol 455:395–417. https://doi.org/10.1016/S0076-6879(08)04214-6
103. Ceres P, Zlotnick A. 2002. Weak protein-protein interactions are sufficient to drive assembly of hepatitis B virus capsids. Biochemistry 41:11525–11531. https://doi.org/10.1021/bi0261645
104. Parent KN, Suhanovsky MM, Teschke CM. 2007. Phage P22 procapsids equilibrate with free coat protein subunits. J Mol Biol 365:513–522. https://doi.org/10.1016/j.jmb.2006.09.088
105. Starr CA, Barnes LF, Jarrold MF, Zlotnick A. 2022. Hysteresis in hepatitis B virus (HBV) requires assembly of near-perfect capsids. Biochemistry 61:505–513. https://doi.org/10.1021/acs.biochem.1c00810
106. Hogle JM. 2002. Poliovirus cell entry: common structural themes in viral cell entry pathways. Annu Rev Microbiol 56:677–702. https://doi.org/10.1146/annurev.micro.56.012302.160757
107. Greber UF, Suomalainen M. 2022. Adenovirus entry: stability, uncoating, and nuclear import. Mol Microbiol 118:309–320. https://doi.org/10.1111/mmi.14909
108. Stray SJ, Bourne CR, Punna S, Lewis WG, Finn MG, Zlotnick A. 2005. A heteroaryldihydropyrimidine activates and can misdirect hepatitis B virus capsid assembly. Proc Natl Acad Sci USA 102:8138–8143. https://doi.org/10.1073/pnas.0409732102
109. Paine AW, Hagan MF, Manoharan VN. 2025. Disassembly of virus-like particles and the stabilizing role of the nucleic acid cargo. J Phys Chem B 129:1516–1528. https://doi.org/10.1021/acs.jpcb.4c07215
110. Axen SD, Erbilgin O, Kerfeld CA. 2014. A taxonomy of bacterial microcompartment loci constructed by a novel scoring method. PLoS Comput Biol 10:e1003898. https://doi.org/10.1371/journal.pcbi.1003898
111. Giessen TW. 2024. The structural diversity of encapsulin protein shells. Chembiochem 25:e202400535. https://doi.org/10.1002/cbic.202400535
112. Nichols RJ, LaFrance B, Phillips NR, Radford DR, Oltrogge LM, Valentin-Alvarado LE, Bischoff AJ, Nogales E, Savage DF. 2021. Discovery and characterization of a novel family of prokaryotic nanocompartments involved in sulfur metabolism. eLife 10:e59288. https://doi.org/10.7554/eLife.59288
113. Sutter M, Boehringer D, Gutmann S, Günther S, Prangishvili D, Loessner MJ, Stetter KO, Weber-Ban E, Ban N. 2008. Structural basis of enzyme encapsulation into a bacterial nanocompartment. Nat Struct Mol Biol 15:939–947. https://doi.org/10.1038/nsmb.1473
114. Berger C, Lewis C, Gao Y, Knoops K, López-Iglesias C, Peters PJ, Ravelli RBG. 2025. *In situ* and *in vitro* cryo-EM reveal structures of mycobacterial encapsulin assembly intermediates. Commun Biol 8:245. https://doi.org/10.1038/s42003-025-07660-5
115. Mohajerani F, Sayer E, Neil C, Inlow K, Hagan MF. 2021. Mechanisms of scaffold-mediated microcompartment assembly and size control. ACS Nano 15:4197–4212. https://doi.org/10.1021/acsnano.0c05715
116. Perlmutter JD, Mohajerani F, Hagan MF. 2016. Many-molecule encapsulation by an icosahedral shell. eLife 5:e14078. https://doi.org/10.7554/eLife.14078
117. Mohajerani F, Hagan MF. 2018. The role of the encapsulated cargo in microcompartment assembly. PLoS Comput Biol 14:e1006351. https://doi.org/10.1371/journal.pcbi.1006351
118. Rotskoff GM, Geissler PL. 2018. Robust nonequilibrium pathways to microcompartment assembly. Proc Natl Acad Sci USA 115:6341–6346. https://doi.org/10.1073/pnas.1802499115
119. Aussignargues C, Paasch BC, Gonzalez-Esquer R, Erbilgin O, Kerfeld CA. 2015. Bacterial microcompartment assembly: the key role of encapsulation peptides. Commun Integr Biol 8:e1039755. https://doi.org/10.1080/19420889.2015.1039755
120. Zarzycki J, Erbilgin O, Kerfeld CA. 2015. Bioinformatic characterization of glycyl radical enzyme-associated bacterial microcompartments. Appl Environ Microbiol 81:8315–8329. https://doi.org/10.1128/AEM.02587-15
121. Kinney JN, Salmeen A, Cai F, Kerfeld CA. 2012. Elucidating essential role of conserved carboxysomal protein CcmN reveals common feature of bacterial microcompartment assembly. J Biol Chem 287:17729–17736. https://doi.org/10.1074/jbc.M112.355305
122. Erbilgin O, Sutter M, Kerfeld CA. 2016. The structural basis of coenzyme a recycling in a bacterial organelle. PLoS Biol 14:e1002399. https://doi.org/10.1371/journal.pbio.1002399
123. Tobimatsu T, Kawata M, Toraya T. 2005. The N-terminal regions of beta and gamma subunits lower the solubility of adenosylcobalamin-dependent diol dehydratase. Biosci Biotechnol Biochem 69:455–462. https://doi.org/10.1271/bbb.69.455
124. Shibata N, Tamagaki H, Hieda N, Akita K, Komori H, Shomura Y, Terawaki S-I, Mori K, Yasuoka N, Higuchi Y, Toraya T. 2010. Crystal structures of ethanolamine ammonia-lyase complexed with coenzyme B12 analogs and substrates. J Biol Chem 285:26484–26493. https://doi.org/10.1074/jbc.M110.125112
125. Trettel DS, López CA, Rodriguez E, Marrone BL, Gonzalez-Esquer CR. 2025. A blueprint for biomolecular condensation driven by bacterial microcompartment encapsulation peptides. Nat Commun 16:7378. https://doi.org/10.1038/s41467-025-62772-0
126. Kerfeld CA, Melnicki MR. 2016. Assembly, function and evolution of cyanobacterial carboxysomes. Curr Opin Plant Biol 31:66–75. https://doi.org/10.1016/j.pbi.2016.03.009
127. Menon BB, Dou Z, Heinhorst S, Shively JM, Cannon GC. 2008. *Halothiobacillus neapolitanus* carboxysomes sequester heterologous and chimeric RubisCO species. PLoS One 3:e3570. https://doi.org/10.1371/journal.pone.0003570
128. Iancu CV, Morris DM, Dou Z, Heinhorst S, Cannon GC, Jensen GJ. 2010. Organization, structure, and assembly of alpha-carboxysomes determined by electron cryotomography of intact cells. J Mol Biol 396:105–117. https://doi.org/10.1016/j.jmb.2009.11.019
129. Dai W, Chen M, Myers C, Ludtke SJ, Pettitt BM, King JA, Schmid MF, Chiu W. 2018. Visualizing individual RuBisCO and its assembly into carboxysomes in marine cyanobacteria by cryo-electron tomography. J Mol Biol 430:4156–4167. https://doi.org/10.1016/j.jmb.2018.08.013
130. Sun Y, Harman VM, Johnson JR, Brownridge PJ, Chen T, Dykes GF, Lin Y, Beynon RJ, Liu L-N. 2022. Decoding the absolute stoichiometric composition and structural plasticity of α-carboxysomes. mBio 13:e0362921. https://doi.org/10.1128/mbio.03629-21
131. Yang M, Wenner N, Dykes GF, Li Y, Zhu X, Sun Y, Huang F, Hinton JCD, Liu LN. 2022. Biogenesis of a bacterial metabolosome for propanediol utilization. Nat Commun 13:2920. https://doi.org/10.1038/s41467-022-30608-w
132. Lehman BP, Chowdhury C, Bobik TA. 2017. The N terminus of the PduB protein binds the protein shell of the Pdu microcompartment to its enzymatic core. J Bacteriol 199:e00785-16. https://doi.org/10.1128/JB.00785-16
133. Zarzycki J, Sutter M, Cortina NS, Erb TJ, Kerfeld CA. 2017. *In vitro* characterization and concerted function of three core enzymes of a glycyl radical enzyme - associated bacterial microcompartment. Sci Rep 7:42757. https://doi.org/10.1038/srep42757
134. Flecken M, Wang H, Popilka L, Hartl FU, Bracher A, Hayer-Hartl M. 2020. Dual functions of a rubisco activase in metabolic repair and recruitment to carboxysomes. Cell 183:457–473. https://doi.org/10.1016/j.cell.2020.09.010
135. Yang M, Adegbite O, Chang P, Cheng J, Wang Y, Held M, Zhu X, Li Y, Dykes GF, Chen Y, Savage N, Zhang YZ, Gao J, Hinton JCD, Lian LY, Liu LN. 2025. Molecular basis of the biogenesis of a protein organelle for ethanolamine utilization. Sci Adv 11:eadx9774. https://doi.org/10.1126/sciadv.adx9774
136. Benjamin J, Ganser-Pornillos BK, Tivol WF, Sundquist WI, Jensen GJ. 2005. Three-dimensional structure of HIV-1 virus-like particles by electron cryotomography. J Mol Biol 346:577–588. https://doi.org/10.1016/j.jmb.2004.11.064
137. Young EJ, Kirst H, Dwyer ME, Vermaas JV, Kerfeld CA. 2025. Quantitative measurement of molecular permeability to a synthetic bacterial microcompartment shell system. ACS Synth Biol 14:1405–1413. https://doi.org/10.1021/acssynbio.4c00290
138. Tefft NM, Yadav NS, Gruenberg Cross MC, Swiggett CD, Parent KN, Vermaas JV, TerAvest MA. 2026. Encapsulation in a bacterial microcompartment shell improves thermal stability of a glycolytic enzyme. bioRxiv. https://doi.org/10.64898/2026.01.28.702358:2026.01.28.702358

139. Hamilton S, Modi T, Šulc P, Banu Ozkan S. 2024. RNA-induced allosteric coupling drives viral capsid assembly. PRX Life 2:013012. https://doi.org/10.1103/prxlife.2.013012
140. Rastandeh A, Makasarashvili N, Dhaliwal HK, Baker S, Subramanian S, Villarreal DA, Gamez EI, Parent KN, Garmann RF. 2025. Measuring the selective packaging of RNA molecules by viral coat proteins in cells. Proc Natl Acad Sci USA 122:e2505190122. https://doi.org/10.1073/pnas.2505190122
141. Crowther RA, Kiselev NA, Bottcher B, Berriman JA, Borisova GP, Ose V, Pumpens P. 1994. Three-dimensional structure of hepatitis B virus core particles determined by electron cryomicroscopy. Cell 77:943–950. https://doi.org/10.1016/0092-8674(94)90142-2
142. Dryden KA, Wieland SF, Whitten-Bauer C, Gerin JL, Chisari FV, Yeager M. 2006. Native hepatitis B virions and capsids visualized by electron cryomicroscopy. Mol Cell 22:843–850. https://doi.org/10.1016/j.molcel.2006.04.025
143. Thuman-Commike PA, Greene B, Malinski JA, King J, Chiu W. 1998. Role of the scaffolding protein in P22 procapsid size determination suggested by T = 4 and T = 7 procapsid structures. Biophys J 74:559–568. https://doi.org/10.1016/S0006-3495(98)77814-2
144. Parent KN, Suhanovsky MM, Teschke CM. 2007. Polyhead formation in phage P22 pinpoints a region in coat protein required for conformational switching. Mol Microbiol 65:1300–1310. https://doi.org/10.1111/j.1365-2958.2007.05868.x
145. Earnshaw W, King J. 1978. Structure of phage P22 coat protein aggregates formed in the absence of the scaffolding protein. J Mol Biol 126:721–747. https://doi.org/10.1016/0022-2836(78)90017-7
146. Parent KN, Sinkovits RS, Suhanovsky MM, Teschke CM, Egelman EH, Baker TS. 2010. Cryo-reconstructions of P22 polyheads suggest that phage assembly is nucleated by trimeric interactions among coat proteins. Phys Biol 7:045004. https://doi.org/10.1088/1478-3975/7/4/045004
147. Suhanovsky MM, Parent KN, Dunn SE, Baker TS, Teschke CM. 2010. Determinants of bacteriophage P22 polyhead formation: the role of coat protein flexibility in conformational switching. Mol Microbiol 77:1568–1582. https://doi.org/10.1111/j.1365-2958.2010.07311.x
148. Noël CR, Cai F, Kerfeld CA. 2016. Purification and characterization of protein nanotubes assembled from a single bacterial microcompartment shell subunit. Adv Materials Inter 3:1500295. https://doi.org/10.1002/admi.201500295
149. Zedler JAZ, Schirmacher AM, Russo DA, Hodgson L, Gundersen E, Matthes A, Frank S, Verkade P, Jensen PE. 2023. Self-assembly of nanofilaments in cyanobacteria for protein co-localization. ACS Nano 17:25279–25290. https://doi.org/10.1021/acsnano.3c08600
150. Sutter M, Faulkner M, Aussignargues C, Paasch BC, Barrett S, Kerfeld CA, Liu LN. 2016. Visualization of bacterial microcompartment facet assembly using high-speed atomic force microscopy. Nano Lett 16:1590–1595. https://doi.org/10.1021/acs.nanolett.5b04259
151. Parsons JB, Frank S, Bhella D, Liang M, Prentice MB, Mulvihill DP, Warren MJ. 2010. Synthesis of empty bacterial microcompartments, directed organelle protein incorporation, and evidence of filament-associated organelle movement. Mol Cell 38:305–315. https://doi.org/10.1016/j.molcel.2010.04.008
152. Wang P, Li J, Li T, Li K, Ng PC, Wang S, Chriscoli V, Basle A, Marles-Wright J, Zhang YZ, Liu LN. 2024. Molecular principles of the assembly and construction of a carboxysome shell. Sci Adv 10:eadr4227. https://doi.org/10.1126/sciadv.adr4227
153. Schmidt-Dannert S, Zhang G, Johnston T, Quin MB, Schmidt-Dannert C. 2018. Building a toolbox of protein scaffolds for future immobilization of biocatalysts. Appl Microbiol Biotechnol 102:8373–8388. https://doi.org/10.1007/s00253-018-9252-6
154. Twarock R. 2006. Mathematical virology: a novel approach to the structure and assembly of viruses. Phil Trans R Soc A 364:3357–3373. https://doi.org/10.1098/rsta.2006.1900